

Triangle Singularity in the Production of $X(3872)$ and a Photon in e^+e^- Annihilation

Eric Braaten,^{*} Li-Ping He,[†] and Kevin Ingles[‡]

Department of Physics, The Ohio State University, Columbus, OH 43210, USA

(Dated: September 4, 2019)

If the $X(3872)$ is a weakly bound charm-meson molecule, it can be produced in e^+e^- annihilation by the creation of $D^{*0}\bar{D}^{*0}$ from a virtual photon followed by the rescattering of the charm-meson pair into X and a photon. A triangle singularity produces a narrow peak in the cross section for $e^+e^- \rightarrow X\gamma$ about 2.2 MeV above the $D^{*0}\bar{D}^{*0}$ threshold. We predict the normalized cross section in the region near the peak. The peak from the triangle singularity may be observable by the BESIII detector.

PACS numbers: 14.80.Va, 67.85.Bc, 31.15.bt

Keywords: Exotic hadrons, charm mesons, effective field theory, triangle singularity.

Since early in this century, a large number of exotic hadrons whose constituents include a heavy quark and its antiquark have been discovered in high energy physics experiments [1–9]. The first on the list of these exotic heavy hadrons is the $X(3872)$ meson, which was discovered in 2003 in exclusive decays of B^\pm mesons into $K^\pm X$ by observing the decay of X into $J/\psi \pi^+\pi^-$ [10]. The J^{PC} quantum numbers of X were eventually determined to be 1^{++} [11]. Its mass is extremely close to the $D^{*0}\bar{D}^0$ threshold, with the difference being only 0.01 ± 0.18 MeV [12]. This suggests that $X(3872)$ is a weakly bound S-wave charm-meson molecule with the flavor structure

$$|X(3872)\rangle = \frac{1}{\sqrt{2}}\left(|D^{*0}\bar{D}^0\rangle + |D^0\bar{D}^{*0}\rangle\right). \quad (1)$$

There are however alternative models for the X [1–8]. The X has been observed in many more decay modes than any of the other exotic heavy hadrons. In addition to $J/\psi \pi^+\pi^-$, it has been observed in $J/\psi \pi^+\pi^-\pi^0$, $J/\psi \gamma$, $\psi(2S)\gamma$, $D^0\bar{D}^0\pi^0$, $D^0\bar{D}^0\gamma$, and most recently $\chi_{c1}\pi^0$ [13]. Despite its observation in 7 different decay modes, a consensus on the nature of X has not been achieved.

There may be aspects of the production of X that are more effective at discriminating between models than the decays of X . One way in which the nature of a hadron can be revealed by its production is through *triangle singularities*. Triangle singularities are kinematic singularities that arise if three virtual particles that form a triangle in a Feynman diagram can all be on their mass shells simultaneously. There have been several previous investigations of the effects of triangle singularities on the production of exotic heavy mesons [14–17]. Guo has recently pointed out that any high-energy process that can create $D^{*0}\bar{D}^{*0}$ at short distances in an S-wave channel will produce $X\gamma$ with a narrow peak near the $D^{*0}\bar{D}^{*0}$ threshold due to a triangle singularity [18]. One such process is electron-positron annihilation, which can create an S-wave $D^{*0}\bar{D}^{*0}$ pair recoiling against a π^0 . Guo suggested that the peak in the line shape for $X\gamma$ due to

the triangle singularity could be used to determine the binding energy of X more accurately than a direct mass measurement.

If the X is a weakly bound charm-meson molecule, it can be produced by any reaction that can produce its constituents $D^{*0}\bar{D}^0$ and $D^0\bar{D}^{*0}$. It can be produced by the creation of $D^{*0}\bar{D}^0$ and $D^0\bar{D}^{*0}$ at short distances of order $1/m_c$, where m_c is the charm quark mass, followed by the binding of the charm mesons into X at longer distances. The X can also be produced by the creation of $D^*\bar{D}^*$ at short distances followed by the rescattering of the charm-meson pair into X and a pion at longer distances [19]. The $D^*\bar{D}^*$ rescattering mechanism predicts that the Dalitz plot from the decay of a B meson into $KX\pi$ should be dominated by a resonance band from the decay into $K^*(892)X$ and a smooth distribution in $X\pi$ invariant mass from the rescattering of $D^*\bar{D}^*$ [20]. The production of X accompanied by a pion from $D^*\bar{D}^*$ rescattering provides an additional production mechanism for X at a high-energy hadron collider that could help explain the large prompt production rate of X that has been observed at the Tevatron and the LHC [19, 21].

The quantum numbers 1^{++} of the X imply that $X\gamma$ can be produced directly by e^+e^- annihilation into a virtual photon. This process can proceed through the creation of $D^{*0}\bar{D}^{*0}$ at short distances in a P-wave channel, followed by the rescattering of the charm-meson pair into $X\gamma$. The production of $X\gamma$ in e^+e^- annihilation near the $D^{*0}\bar{D}^{*0}$ threshold was discussed previously by Dubynskiy and Voloshin [22]. They calculated the absorptive contribution to the cross section from e^+e^- annihilation into on-shell charm mesons $D^{*0}\bar{D}^{*0}$ followed by their rescattering into $X\gamma$. They predicted that the cross section has a peak only a few MeV above the $D^{*0}\bar{D}^{*0}$ threshold, although they did not predict its normalization. In retrospect, this peak comes from a triangle singularity.

In this paper, we calculate the cross section for $e^+e^- \rightarrow X\gamma$ near the $D^{*0}\bar{D}^{*0}$ threshold. We show that the absorptive contribution considered in Ref. [22] is not a good approximation for the cross section. We give a normal-

ized prediction for the cross section by using results from a fit to Belle data on $e^+e^- \rightarrow D^*\bar{D}^*$ by Uglov *et al.* [23]. The peak from the triangle singularity is large enough that it could be observable by the BESIII detector.

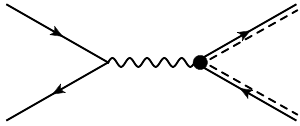


FIG. 1: Feynman diagram for $e^+e^- \rightarrow D^{*0}\bar{D}^{*0}$. The spin-1 charm mesons D^{*0} and \bar{D}^{*0} are represented by double lines consisting of a dashed line and a solid line with an arrow.

A pair of spin-1 charm mesons $D^{*0}\bar{D}^{*0}$ can be produced from the annihilation of e^+e^- into a virtual photon. The Feynman diagram for this process is shown in Fig. 1. We use nonrelativistic normalizations for the charm mesons in the final state. In the center-of-momentum frame, the matrix element has the form

$$\mathcal{M} = -i \frac{e^2}{s} \bar{v} \gamma^i u J^i, \quad (2)$$

where s is the square of the center-of-mass energy, \bar{v} and u are the spinors for the colliding e^+ and e^- , and \mathbf{J} is the matrix element of the electromagnetic current between the QCD vacuum and the $D^{*0}\bar{D}^{*0}$ state. Near the threshold for producing $D^{*0}\bar{D}^{*0}$, the charm-meson pair must be produced in a P-wave state with total spin 0 or 2. The matrix element of the current that creates D^{*0} and \bar{D}^{*0} with momenta $+\mathbf{k}$ and $-\mathbf{k}$ and with polarization vectors $\boldsymbol{\varepsilon}$ and $\bar{\boldsymbol{\varepsilon}}$ can be expressed as $J^i = \mathcal{A}^{ijkl} k^j \varepsilon^{*k} \bar{\varepsilon}^{*l}$. The Cartesian tensor \mathcal{A}^{ijkl} is

$$\mathcal{A}^{ijkl} = A_0 \delta^{ij} \delta^{kl} + \frac{3}{2\sqrt{5}} A_2 \left(\delta^{ik} \delta^{jl} + \delta^{il} \delta^{jk} - \frac{2}{3} \delta^{ij} \delta^{kl} \right), \quad (3)$$

where A_0 and A_2 are amplitudes for creating $D^{*0}\bar{D}^{*0}$ with total spin 0 and 2, respectively. The cross section for e^+e^- annihilation into $D^{*0}\bar{D}^{*0}$ near the threshold is

$$\sigma[e^+e^- \rightarrow D^{*0}\bar{D}^{*0}] = \frac{4\pi\alpha^2 M_{*0}}{s^2} [|A_0|^2 + |A_2|^2] k^3, \quad (4)$$

where M_{*0} is the mass of the D^{*0} and $k = [M_{*0}(\sqrt{s} - 2M_{*0})]^{1/2}$ is the relative momentum of the $D^{*0}\bar{D}^{*0}$ pair.

The Belle collaboration has measured exclusive cross sections for e^+e^- annihilation into several pairs of charm mesons, including $D^{*+}D^{*-}$ [24, 25]. Uglov *et al.* have analyzed the Belle data using a unitary approach based on a coupled channel model [23]. They included a spin-2 F-wave amplitude for $e^+e^- \rightarrow D^*\bar{D}^*$ as well as spin-0 and spin-2 P-wave amplitudes. Near the $D^{*+}D^{*-}$ threshold at 4020.5 MeV, the spin-0 and spin-2 P-wave contributions to the cross sections have the k^3 behavior in Eq. (4). A fit to the two terms in the cross section in Eq. (4), with M_{*0} replaced by the mass M_{*1} of the D^{*+}

and $k = [M_{*1}(\sqrt{s} - 2M_{*1})]^{1/2}$, gives

$$|A_0| = 8 \text{ GeV}^{-1}, \quad |A_2| = 15 \text{ GeV}^{-1}. \quad (5)$$

These coefficients have natural magnitudes of order $1/m_\pi$. The factor $|A_0|^2 + |A_2|^2$ in Eq. (4) is determined more accurately by fitting cross sections than the ratio $|A_2|/|A_0|$.

The values of $|A_0|$ and $|A_2|$ for $e^+e^- \rightarrow D^{*+}D^{*-}$ in Eq. (5) can be inserted into Eq. (4) to predict the cross section for $e^+e^- \rightarrow D^{*0}\bar{D}^{*0}$ near the $D^{*0}\bar{D}^{*0}$ threshold at 4013.7 MeV. This prediction is based on the reasonable assumption that the creation of the charm-meson pair proceeds through the direct coupling of the virtual photon to the charm quark and that the contribution from its direct coupling to the light quark is negligible.

If the $X(3872)$ is a weakly bound charm-meson molecule, its constituents are the superposition of charm mesons in Eq. (1). The reduced mass of $D^{*0}\bar{D}^0$ is $\mu = M_{*0}M_0/(M_{*0} + M_0)$, where M_0 is the mass of the D^0 . The mass difference between the D^{*0} and D^0 is $\delta = M_{*0} - M_0 = 142.0$ MeV. The present value of the difference E_X between the mass of the X and the energy of the $D^{*0}\bar{D}^0$ scattering threshold is [12]

$$E_X \equiv M_X - (M_{*0} + M_0) = (+0.01 \pm 0.18) \text{ MeV}. \quad (6)$$

If this difference is negative, X is a bound state with binding energy $|E_X|$ and binding momentum $\gamma_X = \sqrt{2\mu|E_X|}$. The central value in Eq. (6) corresponds to a charm-meson pair above the scattering threshold. The value lower by 1σ corresponds to a bound state with binding energy $|E_X| = 0.17$ MeV and binding momentum $\gamma_X = 18$ MeV.

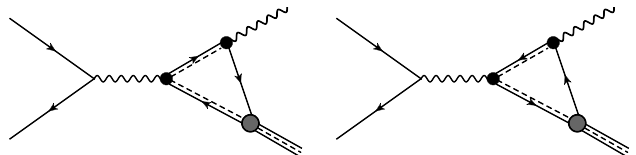


FIG. 2: Feynman diagrams for $e^+e^- \rightarrow \gamma X$ from rescattering of $D^{*0}\bar{D}^{*0}$. The X is represented by a triple line consisting of two solid lines and a dashed line. The spin-0 charm mesons D^0 and \bar{D}^0 are represented by solid lines with an arrow.

The X can be produced in e^+e^- annihilation through the creation of $D^{*0}\bar{D}^{*0}$ by a virtual photon followed by the rescattering of the charm-meson pair into $X\gamma$. The Feynman diagrams for this process are shown in Fig. 2. The vertex for the virtual photon to create D^{*0} and \bar{D}^{*0} with momenta $+\mathbf{k}$ and $-\mathbf{k}$ and vector indices m and n is $e\mathcal{A}^{ijmn}k^j$, where the Cartesian tensor is given in Eq. (3). The vertex for the transition of D^{*0} to $D^0\gamma$ with a photon of momentum \mathbf{k} is $-e\nu\epsilon^{ijm}k^m$, where i is the vector index of D^{*0} . The transition magnetic moment $e\nu$ can be determined from the radiative decay width of D^{*0} [26]: $\nu = 0.95 \text{ GeV}^{-1}$. The binding of $D^{*0}\bar{D}^0$ or $D^0\bar{D}^{*0}$

into X can be described within an effective field theory called XEFT [27, 28]. The vertices for the couplings of $D^{*0}\bar{D}^0$ to X and $D^0\bar{D}^{*0}$ to X can be expressed as $i(\sqrt{\pi}\gamma_X/\mu)\delta^{kl}$, where γ_X is the binding momentum of the X and k and l are the vector indices of the spin-1 charm meson and the X [29].

The matrix element for $e^+e^- \rightarrow X\gamma$ is the sum of the two diagrams in Fig. 2. We use nonrelativistic propagators for the charm mesons. The matrix element for producing X and γ with momenta \mathbf{q} and $-\mathbf{q}$ and with polarization vectors $\boldsymbol{\epsilon}_X$ and $\boldsymbol{\epsilon}_\gamma$ can be expressed as

$$\mathcal{M} = \frac{2e^3\nu M_{*0}M_0}{s\mu} \bar{v}\gamma^i u \mathcal{J}^i F(W). \quad (7)$$

The current \mathcal{J}^i is

$$\mathcal{J} = \left(A_0 - \frac{1}{\sqrt{5}}A_2 \right) (\hat{\mathbf{q}} \times \boldsymbol{\epsilon}_\gamma \cdot \boldsymbol{\epsilon}_X) \hat{\mathbf{q}} + \frac{3}{2\sqrt{5}}A_2 (\hat{\mathbf{q}} \cdot \boldsymbol{\epsilon}_X) \hat{\mathbf{q}} \times \boldsymbol{\epsilon}_\gamma. \quad (8)$$

The scalar loop amplitude $F(W)$ is a function of the center-of-mass energy $W = \sqrt{s} - 2M_{*0}$ relative to the $D^{*0}\bar{D}^{*0}$ threshold. It can be calculated analytically by integrating over the loop energy using a contour integral around the pole of one propagator, combining the remaining two propagators with a Feynman parameter x , integrating over the loop momentum, and finally integrating over x :

$$F(W) = -i \frac{\mu\sqrt{\pi}\gamma_X}{4\pi M_0} q \left(\frac{B^2 - A^2 - C^2}{2C^2} \log \frac{A+B+C}{A+B-C} + \frac{A-B}{C} \right), \quad (9)$$

where

$$A = \sqrt{k^2 + iM_{*0}\Gamma_{*0}}, \quad (10a)$$

$$B = i\sqrt{\gamma_X^2 - i\mu\Gamma_{*0}}, \quad (10b)$$

$$C = (\mu/M_0)q, \quad (10c)$$

and $\Gamma_{*0} = 56$ keV is the predicted width of the D^{*0} [26]. The dependence on W is through $k^2 = M_{*0}W$ and the momentum q of X , which is equal to the energy of the photon and is determined by energy conservation:

$$W = q - \delta + \frac{q^2}{2M_X} - \frac{\gamma_X^2}{2\mu}. \quad (11)$$

The loop amplitude in Eq. (9) has a triangle singularity in the limit where the binding energy of X is 0 and the decay width of the D^{*0} is 0. The singularity arises from the integration region where the three charm mesons whose lines form triangles in the diagrams in Fig. 2 are all on their mass shells simultaneously. The two charm mesons that become constituents of the X are both on their mass shells in the limit where the binding energy is 0. There is a specific energy W_Δ where the spin-1 charm meson

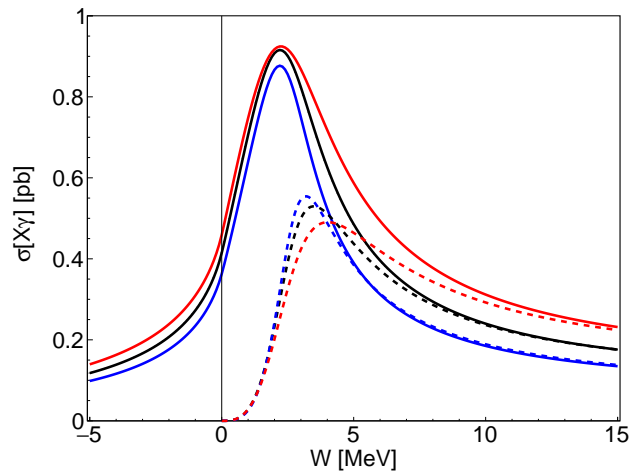


FIG. 3: Cross section for $e^+e^- \rightarrow X(3872)\gamma$ as a function of the center-of-mass energy W relative to the $D^{*0}\bar{D}^{*0}$ threshold. The solid curves in order of decreasing cross sections are for binding energies $|E_X| = 0.30$ MeV, 0.17 MeV, and 0.10 MeV. The dashed curves are the absorptive contributions, which approach the corresponding cross sections as W increases.

that emits the photon can also be on its mass shell. The triangle singularity is a logarithmic divergence of Eq. (9) in the limits $\gamma_X \rightarrow 0$ and $\Gamma_{*0} \rightarrow 0$. In these limits, the denominator of the argument of the logarithm is zero at the energy for which $k = (\mu/M_0)q$. The energy W_Δ can be obtained by solving this equation for W using Eq. (11) for q . A simple approximation to the solution for W is

$$W_\Delta = (\mu/M_0)^2\delta^2/M_{*0}. \quad (12)$$

The predicted energy is $W_\Delta = 2.7$ MeV.

The cross section for e^+e^- annihilation into $X\gamma$ at center-of-mass energy near the $D^{*0}\bar{D}^{*0}$ threshold is

$$\sigma[e^+e^- \rightarrow X\gamma] = \frac{128\pi^2\alpha^3\nu^2 M_X^2}{3s^2(1+q/M_X)} \times \left(\left| A_0 - \frac{1}{\sqrt{5}}A_2 \right|^2 + \frac{9}{20}|A_2|^2 \right) q |F(W)|^2. \quad (13)$$

We have used nonrelativistic phase space for X and relativistic phase space for the photon. The factor that depends on A_0 and A_2 differs from $|A_0|^2 + |A_2|^2$ by a multiplicative factor that depends on A_2/A_0 and can range from 0.34 to 1.31.

The cross section for $e^+e^- \rightarrow X\gamma$ in Eq. (13) near the $D^{*0}\bar{D}^{*0}$ threshold is shown in Fig. 3 for three values of the binding energy: $|E_X| = 0.30$ MeV, 0.17 MeV, and 0.10 MeV. For smaller values of E_X , the line shape becomes sensitive to the unknown decay width of X . It is necessary to take into account the imaginary part of γ_X , and it becomes increasingly difficult to accommodate the significant branching fraction into $J/\psi\pi^+\pi^-$ [30]. We have chosen the value of A_2/A_0 that maximizes the

normalization factor in the cross section given the value $|A_0|^2 + |A_2|^2 = 280 \text{ GeV}^{-2}$ from Eq. (5). The minimum normalization factor is smaller by a factor of 3.8. The cross section has a narrow peak produced by the triangle singularity. The position of the peak, which is insensitive to the binding energy, is 2.2 MeV above the $D^{*0}\bar{D}^{*0}$ threshold, near the prediction from Eq. (12). The height of the peak is also insensitive to $|E_X|$. The full width at half maximum is 5.1 MeV at $|E_X| = 0.17 \text{ MeV}$, and it decreases as $|E_X|$ decreases. Beyond the peak, the cross section decreases to a local minimum at an energy W near 40 MeV, before increasing because of the k^3 dependence of the P-wave cross section for producing $D^{*0}\bar{D}^{*0}$. The minimum is 0.1 pb for $|E_X| = 0.17 \text{ MeV}$.

The loop amplitude $F(W)$ in Eq. (9) has an absorptive contribution that corresponds to e^+e^- annihilation into on-shell charm mesons $D^{*0}\bar{D}^{*0}$ followed by the rescattering of the charm mesons into $X\gamma$. The absorptive contribution to $F(W)$ is the imaginary part of Eq. (9) in the limit $\Gamma_{*0} \rightarrow 0$:

$$\text{Im}[F(W)] = \frac{\sqrt{\pi\gamma_X}}{4\pi} k \left(\frac{(\mu/M_0)^2 q^2 + k^2 + \gamma_X^2}{4(\mu/M_0)qk} \times \log \frac{[(\mu/M_0)q + k]^2 + \gamma_X^2}{[(\mu/M_0)q - k]^2 + \gamma_X^2} - 1 \right). \quad (14)$$

The absorptive contribution to the cross section, which is obtained by replacing $F(W)$ in Eq. (13) by $\text{Im}[F(W)]$ in Eq. (14), is shown in Fig. 3 for three values of $|E_X|$. The absorptive contribution is zero below the $D^{*0}\bar{D}^{*0}$ threshold. For $|E_X| = 0.17 \text{ MeV}$, the position of the peak in the absorptive contribution is 1.3 MeV higher than that of the full cross section. The height of the peak is 58% of that of the full cross section. Thus the absorptive contribution is not a good approximation to the cross section in the triangle singularity region. At larger energies, the absorptive contribution quickly approaches the full cross section.

In the limit $\Gamma_{*0} \rightarrow 0$, the loop amplitude can be expressed as the momentum integral

$$F(W) = -\frac{1}{\sqrt{2}M_X} \int \frac{d^3k}{(2\pi)^3} \frac{(\mathbf{q} \cdot \mathbf{k}) \psi_X(|\mathbf{k} - (\mu/M_0)\mathbf{q}|)}{W - \mathbf{k}^2/M_{*0} + i\epsilon}, \quad (15)$$

where $\psi_X(k)$ is the universal momentum-space Schrödinger wavefunction for a weakly-bound S-wave molecule normalized so $\int d^3k/(2\pi)^3 |\psi(k)|^2 = 1$. In the rest frame, this wavefunction as a function of the relative momentum k is

$$\psi_X(k) = \frac{\sqrt{8\pi\gamma_X}}{k^2 + \gamma_X^2}. \quad (16)$$

The wavefunction in the integrand of Eq. (15) is in a moving frame where the bound state has momentum \mathbf{q} . It has a maximum as function of \mathbf{k} when the two constituents have equal velocities.

In Ref. [22], Dubynskiy and Voloshin (DV) calculated the absorptive contribution to the cross section for $e^+e^- \rightarrow X\gamma$ using a wavefunction that reduces in the rest frame to

$$\psi_{\text{DV}}(k) = \frac{\sqrt{8\pi\gamma_X\Lambda(\Lambda+\gamma_X)}}{\Lambda - \gamma_X} \left(\frac{1}{k^2 + \gamma_X^2} - \frac{1}{k^2 + \Lambda^2} \right), \quad (17)$$

where Λ is an adjustable parameter. The DV wavefunction was used previously by Voloshin in a study of the decays of $X(3872)$ into $D^0\bar{D}^0\gamma$ [31]. Voloshin identified the parameter γ_X in Eq. (17) with the binding momentum of X . This identification can be justified rigorously only in the limit $\Lambda \rightarrow \infty$ in which the wavefunction reduces to that in Eq. (16). The subtraction in the DV wavefunction in Eq. (17) makes it decrease as $1/k^4$ when k is much larger than the momentum scale Λ . In Ref. [22], DV illustrated their results using the values $\Lambda = 200 \text{ MeV}$ and $\Lambda = 300 \text{ MeV}$. For the wavefunction in the moving frame, DV used $\psi_{\text{DV}}(|\mathbf{k} - \frac{1}{2}\mathbf{q}|)$. It has a maximum as function of \mathbf{k} when the two constituents have equal momenta. Since $\mu/M_0 = 0.518$ is close to $\frac{1}{2}$, the different prescription for the wavefunction in the moving frame has a small effect on the cross section. The subtraction in Eq. (17) also has a small effect in the triangle singularity region.

The BESIII collaboration has measured the cross section for e^+e^- annihilation into $X\gamma$ at center-of-mass energies ranging from 4.008 GeV to 4.6 GeV by observing X in the final states $J/\psi\pi^+\pi^-$ and $J/\psi\omega$ [32, 33]. They did not measure the cross section at energies between 4.009 GeV and 4.178 GeV, which includes the energy 4.016 GeV of the peak from the triangle singularity. The BESIII collaboration measured the cross section in 10 MeV steps between 4.178 GeV and 4.278 GeV [33]. The largest value of the product $\text{Br}\sigma$ of the cross section and the branching fraction into $J/\psi\pi^+\pi^-$ was about 0.5 pb. Upper and lower bounds can be put on the branching fraction Br for the decay of X into $J/\psi\pi^+\pi^-$: $4\% < \text{Br} < 33\%$ [34]. Thus the height of the peak from the triangle singularity at 4.016 GeV could be a significant fraction of the cross section measured in this higher energy region.

Our predictions for the $X + \gamma$ peak from the triangle singularity are based on the assumption that the X is a weakly-bound charm meson molecule whose decay width is smaller than its binding energy. If the decay width is larger than the binding energy or if the X is instead a virtual state, our assumption that it couples to the charm mesons through a momentum-independent vertex breaks down. This could have a significant effect on the peak. The peak could also be modified if there is a multiple fine tuning of hadronic physics that produces a zero or an additional pole in the scattering amplitude for the charm mesons near threshold.

We have pointed out that a triangle singularity produces a narrow peak in the cross section for e^+e^- an-

annihilation into $X\gamma$ at an energy about 2.2 MeV above the $D^{*0}\bar{D}^{*0}$ threshold. We gave a normalized prediction for the cross section in that region. The peak from the triangle singularity is large enough that it could be observable by the BESIII detector. The observation of this peak would provide strong support for the identification of the $X(3872)$ as a weakly bound charm-meson molecule.

This work was supported in part by the Department of Energy under Grant No. de-sc0011726, and by the National Science Foundation under Grant No. PHY-1607190.

* Electronic address: braaten.1@osu.edu

† Electronic address: he.1011@buckeyemail.osu.edu

‡ Electronic address: ingles.27@buckeyemail.osu.edu

- [1] H.X. Chen, W. Chen, X. Liu and S.L. Zhu, The hidden-charm pentaquark and tetraquark states, *Phys. Rept.* **639**, 1 (2016) [arXiv:1601.02092].
- [2] A. Hosaka, T. Iijima, K. Miyabayashi, Y. Sakai and S. Yasui, Exotic hadrons with heavy flavors: X , Y , Z , and related states, *PTEP* **2016**, 062C01 (2016) [arXiv:1603.09229].
- [3] R.F. Lebed, R.E. Mitchell and E.S. Swanson, Heavy-Quark QCD Exotica, *Prog. Part. Nucl. Phys.* **93**, 143 (2017) [arXiv:1610.04528].
- [4] A. Esposito, A. Pilloni and A.D. Polosa, Multi-quark Resonances, *Phys. Rept.* **668**, 1 (2016) [arXiv:1611.07920].
- [5] F.K. Guo, C. Hanhart, U.G. Meißner, Q. Wang, Q. Zhao and B.S. Zou, Hadronic molecules, *Rev. Mod. Phys.* **90**, 015004 (2018) [arXiv:1705.00141].
- [6] A. Ali, J.S. Lange and S. Stone, Exotics: Heavy Pentaquarks and Tetraquarks, *Prog. Part. Nucl. Phys.* **97**, 123 (2017) [arXiv:1706.00610].
- [7] S.L. Olsen, T. Skwarnicki and D. Zieminska, Nonstandard heavy mesons and baryons: Experimental evidence, *Rev. Mod. Phys.* **90**, 015003 (2018) [arXiv:1708.04012].
- [8] M. Karliner, J.L. Rosner and T. Skwarnicki, Multi-quark States, *Ann. Rev. Nucl. Part. Sci.* **68**, 17 (2018) [arXiv:1711.10626].
- [9] C.Z. Yuan, The XYZ states revisited, *Int. J. Mod. Phys. A* **33**, 1830018 (2018) [arXiv:1808.01570].
- [10] S.K. Choi *et al.* [Belle Collaboration], Observation of a narrow charmonium-like state in exclusive $B^\pm \rightarrow K^\pm \pi^+ \pi^- J/\psi$ decays, *Phys. Rev. Lett.* **91**, 262001 (2003) [hep-ex/0309032].
- [11] R. Aaij *et al.* [LHCb Collaboration], Determination of the $X(3872)$ meson quantum numbers, *Phys. Rev. Lett.* **110**, 222001 (2013) [arXiv:1302.6269].
- [12] M. Tanabashi *et al.* [Particle Data Group], Review of Particle Physics, *Phys. Rev. D* **98**, 030001 (2018).
- [13] M. Ablikim *et al.* [BESIII Collaboration], Observation of the decay $X(3872) \rightarrow \pi^0 \chi_{c1}(1P)$, *Phys. Rev. Lett.* **122**, 202001 (2019) [arXiv:1901.03992].
- [14] A.P. Szczepaniak, Triangle Singularities and XYZ Quarkonium Peaks, *Phys. Lett. B* **747**, 410 (2015) [arXiv:1501.01691].
- [15] X.H. Liu, M. Oka and Q. Zhao, Searching for observable effects induced by anomalous triangle singularities, *Phys. Lett. B* **753**, 297 (2016) [arXiv:1507.01674].
- [16] A.P. Szczepaniak, Dalitz plot distributions in presence of triangle singularities, *Phys. Lett. B* **757**, 61 (2016) [arXiv:1510.01789].
- [17] F. K. Guo, Traps in hadron spectroscopy: Thresholds, triangle singularities, ..., *PoS Hadron* **2017**, 015 (2018) [arXiv:1712.10126].
- [18] F.K. Guo, Novel method for precisely measuring the $X(3872)$ mass, *Phys. Rev. Lett.* **122**, 202002 (2019) [arXiv:1902.11221].
- [19] E. Braaten, L.-P. He and K. Ingles, Predictive Solution to the $X(3872)$ Collider Production Puzzle, arXiv:1811.08876 [hep-ph].
- [20] E. Braaten, L.-P. He and K. Ingles, Production of $X(3872)$ Accompanied by a Pion in B Meson Decay arXiv:1902.03259 [hep-ph].
- [21] E. Braaten, L.-P. He and K. Ingles, Production of $X(3872)$ Accompanied by a Pion at Hadron Colliders, arXiv:1903.04355 [hep-ph].
- [22] S. Dubynskiy and M.B. Voloshin, $e^+e^- \rightarrow \gamma X(3872)$ near the $D^*\bar{D}^*$ threshold, *Phys. Rev. D* **74**, 094017 (2006) [hep-ph/0609302].
- [23] T.V. Uglov, Y.S. Kalashnikova, A.V. Nefediev, G.V. Pakhlova and P.N. Pakhlov, Exclusive open-charm near-threshold cross sections in a coupled-channel approach, *JETP Lett.* **105**, 1 (2017) [arXiv:1611.07582].
- [24] K. Abe *et al.* [Belle Collaboration], Measurement of the near-threshold $e^+e^- \rightarrow D^{(*)\pm} D^{(*)\mp}$ cross section using initial-state radiation, *Phys. Rev. Lett.* **98**, 092001 (2007) [hep-ex/0608018].
- [25] G. Pakhlova *et al.* [Belle Collaboration], Measurement of the near-threshold $e^+e^- \rightarrow D\bar{D}$ cross section using initial-state radiation, *Phys. Rev. D* **77**, 011103 (2008) [arXiv:0708.0082].
- [26] J.L. Rosner, Hadronic and radiative D^* widths, *Phys. Rev. D* **88**, 034034 (2013) [arXiv:1307.2550].
- [27] S. Fleming, M. Kusunoki, T. Mehen and U. van Kolck, Pion interactions in the $X(3872)$, *Phys. Rev. D* **76**, 034006 (2007) [hep-ph/0703168].
- [28] E. Braaten, Galilean-invariant effective field theory for the $X(3872)$, *Phys. Rev. D* **91**, 114007 (2015) [arXiv:1503.04791].
- [29] E. Braaten, H.-W. Hammer and T. Mehen, Scattering of an Ultrasoft Pion and the $X(3872)$, *Phys. Rev. D* **82**, 034018 (2010) [arXiv:1005.1688].
- [30] E. Braaten and M. Lu, Line shapes of the $X(3872)$, *Phys. Rev. D* **76**, 094028 (2007) [arXiv:0709.2697].
- [31] M.B. Voloshin, $X(3872)$ diagnostics with decays to $D\bar{D}\gamma$, *Int. J. Mod. Phys. A* **21**, 1239 (2006) [hep-ph/0509192].
- [32] M. Ablikim *et al.* [BESIII Collaboration], Observation of $e^+e^- \rightarrow \gamma X(3872)$ at BESIII, *Phys. Rev. Lett.* **112**, 092001 (2014) [arXiv:1310.4101].
- [33] M. Ablikim *et al.*, Study of $e^+e^- \rightarrow \gamma \omega J/\psi$ and Observation of $X(3872) \rightarrow \omega J/\psi$, *Phys. Rev. Lett.* **122**, 232002 (2019) [arXiv:1903.04695].
- [34] E. Braaten, L. P. He and K. Ingles, Branching Fractions of the $X(3872)$, arXiv:1908.02807 [hep-ph].